

Accelerating Transfer Learning with Near-Data Computation on Cloud Object Stores

Arsany Guirguis*
EPFL

Diana Petrescu*
EPFL

Do Le Quoc
Huawei

Javier Picorel
Huawei

Rachid Guerraoui
EPFL

Florin Dinu
Huawei

ABSTRACT

Near-data computation techniques have been successfully deployed to mitigate the cloud network bottleneck between the storage and compute tiers. At Huawei, we are currently looking to get more value from these techniques by broadening their applicability. Machine learning (ML) applications are an appealing and timely target.

This paper describes our experience applying near-data computation techniques to transfer learning (TL), a widely popular ML technique, in the context of disaggregated cloud object stores. Our techniques benefit both cloud providers and users. They improve our operational efficiency while providing users the performance improvements they demand from us. The main practical challenge to consider is that the storage-side computational resources are limited. Our approach is to split the TL deep neural network (DNN) during the feature extraction phase, before the training phase. This reduces the network transfers to the compute tier and further decouples the batch size of feature extraction from the training batch size. This facilitates our second technique, storage-side batch adaptation, which enables increased concurrency in the storage tier while avoiding out-of-memory errors.

Guided by these insights, we present HAPI, our processing system for TL that spans the compute and storage tiers while remaining transparent to the user. Our evaluation with several state-of-the-art DNNs, such as ResNet, VGG, and Transformer, shows up to 11× improvement in application runtime and up to 8.3× reduction in the data transferred from the storage to the compute tier compared to running the computation entirely in the compute tier.

1 INTRODUCTION

This paper presents our experience applying near-data computation techniques, in the context of cloud object stores, to transfer learning (TL) [69] applications for the benefit of both cloud providers and users. We focus on TL, because it is a widely popular ML technique [14] with a wide range of applications ranging from language models [7, 60], self-driving cars [12] to healthcare [52]. TL allows knowledge in one task to be reused in a different but related task while training with a new dataset. This makes TL the very embodiment of the promise of the cloud. Users who otherwise lack powerful or large-scale storage and compute can build on pre-trained models and popular datasets to obtain state-of-the-art results. As providers are offering the complete ML life-cycle as a service, TL is an indispensable component [4, 17] while cloud object stores (COS) are key to storing the ever larger datasets [3].

All major cloud providers offer cloud object storage solutions (e.g., Huawei OBS [32], Amazon S3 [1], Google Cloud Storage [23],

Azure Blob Storage [8]). Storage disaggregation (i.e., the separation of the storage and compute tiers) is a cornerstone of the object store design, bringing significant operational and financial advantages for providers. Unfortunately, these benefits come with an inherent network bottleneck [2, 65, 67]. This bottleneck will aggravate in the future as storage tiers host increasingly larger data sizes and as storage bandwidth improvements continue to outpace improvements in network bandwidth and compute throughput [20, 62]. To mitigate this network bottleneck, providers have deployed near-data computations techniques which involve provisioning some compute resources alongside the storage tier to run part of an application (called a *pushdown*), essentially to reduce the amount of data transferred to the compute tier. Following the initial success of these techniques on a restricted set of workloads (e.g., SQL), at Huawei we are looking for added value by broadening their applicability to other classes of popular applications. ML applications are a very appealing and timely target.

Applying near-data computation techniques to TL benefits both providers and users. On the one hand, as a cloud provider, we are interested mostly in improving resource efficiency and lowering total cost of ownership (TCO). On the other hand, our customers expect top performance, which for TL translates into shorter training times. To obtain these benefits, we need to overcome a number of practical challenges. Most importantly, the computational resources next to storage are limited because they are only meant to mitigate the network bottleneck and not replace the compute tier. A full-fledged compute tier inside the storage would negate all the benefits of disaggregation. Therefore using these resources efficiently is key. Second, the network between the storage and the compute tiers may still end up limiting performance [39, 50] so reducing the size of network transfers is still important. As we will show, particularly for TL, these two challenges can be contradicting so balancing them carefully is important.

The key to successfully applying near-data computation techniques to TL lies in the unique structure of TL’s fine-tuning phase. Fine-tuning¹ comprises processing a deep neural network (DNN) whose first part performs feature extraction while the latter part performs the actual training (see Figure 1b). Our approach is to carefully split the TL DNN used for fine-tuning such that the feature extraction phase is pushed down, partially or entirely, to the COS. The compute tier executes the training phase and potentially the latter part of the feature extraction phase. This approach to splitting reduces network transfers and has a crucial consequence: it naturally decouples the batch size of feature extraction from the training batch size. The user controls the latter and the provider the former.

¹TL also includes a pre-training phase (§2.3 and Figure 1a), but it is outside the scope of our paper as users often use pre-trained models from the literature.

*The authors had equal contribution.

This decoupling exposes opportunities for improving system efficiency. Specifically, it gives the provider flexibility during feature extraction, where we propose a dynamic batch size adaptation approach that can increase concurrency inside the COS, improving provider-centric metrics such as resource (e.g., GPU memory) usage and compute throughput while avoiding the out-of-memory (OOM) errors that plague ML practitioners. This adaptation does not affect training accuracy. Only the training batch size, which we leave untouched, influences training accuracy.

To the best of our knowledge, we are the first to propose splitting an ML computation between the compute tier and the COS. Our approach to DNN splitting is guided by our detailed per-layer measurement study (§3). We use the insight that layer output sizes decrease non-monotonically, so it is often possible to split early in the DNN at a layer with a comparatively smaller output size. This navigates the two conflicting challenges. On the one hand, minimizing the amount of data sent over the bottleneck network reduces training latency. On the other hand, one should efficiently use the precious computational capabilities of the COS by avoiding pushing down more computation than necessary. The two insights may conflict because, in general, the first layers of the fine-tuning DNNs have the larger output sizes.

We combine our splitting and batch adaptation algorithms into HAPI², our processing system for TL that spans both the COS and compute tiers, is transparent to the user, relies only on very inexpensive profiling runs, and enables even low-end CPU-only users to contribute. HAPI’s design uses a stateless storage-side component alongside lightweight request between the two tiers to simplify practical concerns regarding load balancing, scalability and failure resilience.

Specifically, the contributions of this paper are:

- (1) Identifying and illustrating the benefits, for both users and providers, of applying near-data computation technique to TL on top of COS.
- (2) A per-layer measurement study of TL applications’ runtime, per-layer output size, and GPU memory usage (§3).
- (3) An end-to-end system comprising two key design techniques: DNN splitting (§4.4) and storage-side batch adaptation (§4.5) which reduce network transfers and enable increased concurrency in the COS, respectively.
- (4) An extensive evaluation in Huawei Cloud (§5) with state-of-the-art models, including ResNet [27], VGG [56], and Transformer [59], showing up to 11× improvement in application runtime and up to 8.3× reduction in data transferred between the COS and the compute tier, compared to running TL entirely in the compute tier while enabling 100% use of the GPU memory. Compared to running TL entirely in the COS, HAPI improves throughput by 4.9×.

2 BACKGROUND

2.1 Cloud object stores

Cloud object stores (COS), such as Huawei OBS [32], Amazon S3 [1], Google Cloud Storage [23], and Azure Blob Storage [8], are a popular way to store large-scale unstructured data, providing ease of use, high availability, high scalability, and durability at a low cost [44].

²[https://en.wikipedia.org/wiki/Hapi_\(Nilegod\)](https://en.wikipedia.org/wiki/Hapi_(Nilegod))

COS are the prime example of storage-disaggregation. The COS is connected to the compute tier by a network that, unfortunately, is a bottleneck [20, 39, 40, 50] even when the network is maxed out. The reason are hardware trends. The network bandwidth between the COS and the compute tier is lower than the internal storage bandwidth of COS servers and also lower than the computation throughput [20, 43]. The typical network bandwidth of a single cloud server is 25-100Gbps (3.125-12.5Gbps) [20, 31, 63]. A single modern NVMe SSD can read sequentially at well over 5GBps [53], so 3 NVMe SSDs are sufficient to max out the network bandwidth. In practice, storage servers are provisioned with many more SSDs. Other storage media are faster than SSDs, further aggravating the network bottleneck. With sufficient thread parallelism, DRAM reads can exceed 100Gbps, and persistent memory reads can exceed 30Gbps [64], well above the network bandwidth. Compute throughput also exceeds network bandwidth [20, 43]. Multi-tenancy further degrades the network bandwidth available to a single storage server. All in all, studies [39, 50] have reported read throughput as low as 100Mbps per connection.

In light of this enduring network bottleneck, an important trend has been to push down computation inside the COS, to reduce the amount of data sent over the network. Pushdowns were initially restricted to a subset of SQL (e.g., Amazon S3 Select [6]), but there is a renewed effort in the industry to support more complex pushdowns for computations such as image processing [13] or analytics [2]. At Huawei, we are currently focusing on pushing down parts of ML computations to the COS. This trend goes hand-in-hand with another development, enabling pushdowns to use specialized hardware (§2.2).

Despite these trends, two challenges remain for COS users. The network may still be the bottleneck despite the pushdowns, and the COS computational resources are scarce and need to be used efficiently because they are only meant to mitigate the network bottleneck and not replace the compute tier.

2.2 Hardware-accelerated pushdowns

Pushdowns were initially restricted to a subset of SQL, including filtering, projecting, and aggregation (e.g., Amazon S3 Select [6]). The current, natural trend is to offer the benefits of pushing down to a wider range of applications. Unfortunately, restricting pushdowns to CPUs can lead to wasted resources and performance. First, for more complex operations, CPUs can become a bottleneck. Studies show that even with 32 cores, an SGD optimizer can bottleneck the CPU when using a 100Gbps network [36]. Second, it is not sufficient for the CPU processing to be just faster than the network because the output of a pushdown may be smaller than its input. For a pushdown to generate an output at 12.5Gbps (\approx 100Gbps), assuming an input/output ratio of 2, it needs to process input at 25Gbps. Finally, the aggregate storage bandwidth of a storage server tends to increase faster than CPU capabilities [62].

As a result, the current trend is to allow pushdowns to use specialized hardware such as GPUs. Several works [9, 25] have proposed to use them in storage systems to speed up erasure coding. IBM is offering high-performance storage with NVIDIA GPUs [33, 34]. Finally, there is a push to more-closely integrate storage with GPUs [42, 48], which further increases the appeal of next-to-storage GPUs.

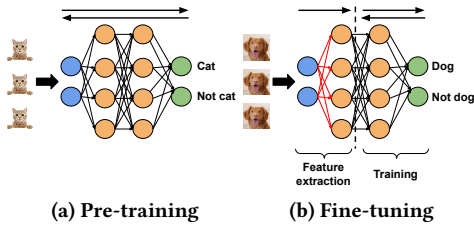


Figure 1: Overview of TL. Top arrows show *forward* and *backward* pass. This paper analyzes the fine-tuning phase. Weights in red are frozen (do not change during fine-tuning).

2.3 Transfer learning

Transfer learning (TL) adapts a pre-trained model on one task with a large amount of data to a similar task [61] by transferring common model features. In doing so it reduces DNN training time and the generalization error [22] (p. 536). Figure 1 illustrates the process. The first part (i.e., *pre-training*, Figure 1a) is outside the scope of this paper and often occurs on a different system. To solve a new task, TL *fine-tunes* the pre-trained model (Figure 1b). Fine-tuning can be divided further into two phases: (i) *feature extraction*, to extract the features from new input data using (partially or entirely) the pre-trained model, and then (ii) *training*, to create a new classifier using the extracted features [22]. Typically, the first few layers of the pre-trained model are frozen during the fine-tuning process, i.e., the model weights of these layers (in red in Figure 1b) are not updated with backpropagation. Every iteration (i.e., input batch processed) involves feature extraction followed by training. We call the last layer of the feature extraction phase the *freeze layer (or index)*.

3 MEASUREMENT STUDY

Next, we present a detailed measurement study of four vision DNNs (AlexNet [41], ResNet18 [27], VGG11 [56], DenseNet121 [29]) and several input datasets. Details about each DNN are shown in Table 1. We characterize the per-layer properties across three dimensions: output size, compute time, and maximum GPU memory used.

Hardware setup. For this section we use two identical GPU-accelerated machines (pi2.4xlarge.4) from the Huawei cloud, one for the HAPI client and the other for the COS and the HAPI server. Each machine has an Intel Xeon Gold 6278C CPU with 16 cores, 64 GBs RAM, 2 Tesla T4 GPUs (16 GB RAM each), and a 300GB SSD and runs Ubuntu 20.04 server 64bit with Tesla Driver 460.73.01 and CUDA 10.2. In some experiments, we use CPU-only clients that have no access to the GPUs. With GPU-based clients, the application runs on both GPUs. The network bandwidth is around 12 Gbps. The freeze layers used are in Table 1.

3.1 Per-layer output size

Figure 2 compares the application input size of 3 datasets, Imagenet [18], iNaturalist [58], and PlantLeaves [55], with the per-layer output sizes. We show a batch size of 1, one input image transformed through the DNN. One can accurately extrapolate from this by multiplying by a specific batch size.

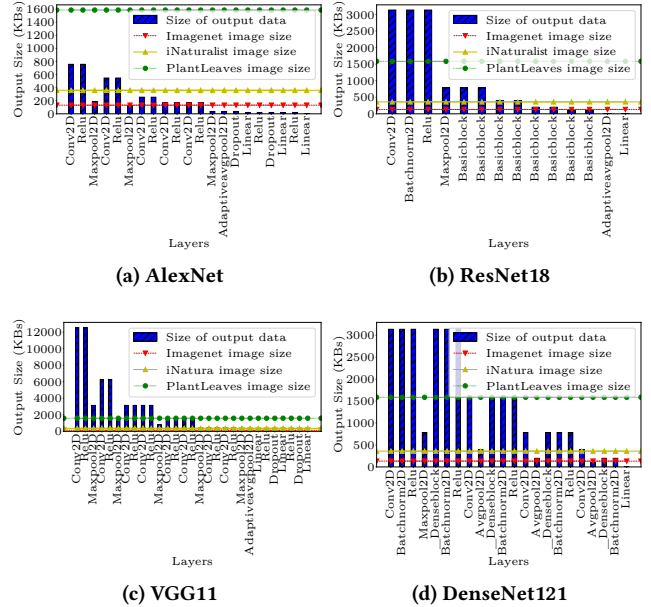


Figure 2: Layer output sizes. Dataset: Synthetic. Batch size=1.

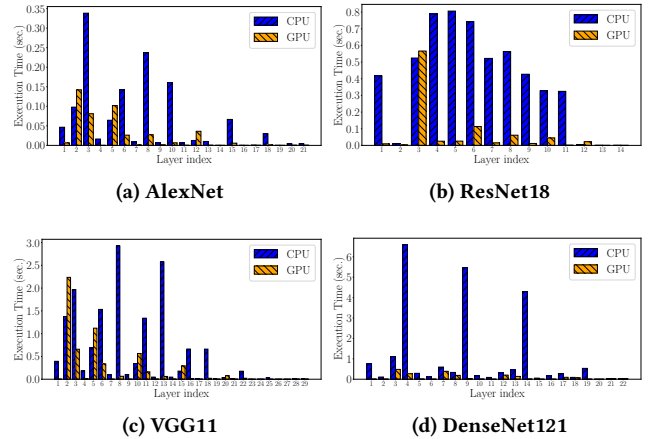


Figure 3: Computation time of the forward pass per layer on both CPU and GPU. Dataset: Synthetic. Batch size = 200.

A critical insight can be derived: for all models, we can find early on in the DNN structure, layers that have output size comparable or smaller than the application input size. These layers are good candidates for splitting the TL application between the COS and the compute tier. The layer output size generally increases in the beginning (with convolution layers) and then decreases (with pooling layers) but not in a monotonic fashion.

3.2 Per-layer computation time

Figure 3 shows the per-layer computation time for the forward pass on CPU and GPU. For all models, earlier layers are more

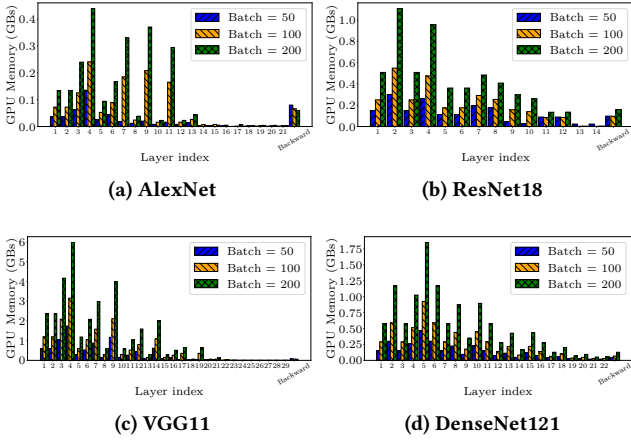


Figure 4: Maximum GPU memory used. Dataset: Synthetic.

computationally expensive. The pattern of the variation is model-dependent. Moreover, as expected, the computation on the CPU generally takes significantly more time. The important exception is the last few layers where there is very little difference between runtime on CPU and GPU. Even more, for some of the later layers, executing on CPU is actually more efficient. This suggests that even clients with a low-end hardware configuration can contribute by executing the last part of the DNN.

3.3 Batch size vs per-layer memory usage

Figure 4 shows the maximum amount of GPU memory utilized per layer for the forward pass over all layers in the DNN. It also shows (right side of each sub-figure) the maximum amount of memory used across all the layers participating in the backward pass. For each model, the backward phase ends at the corresponding freeze index listed in Table 1. For the forward pass, the memory is mainly composed of the intermediate outputs. For the backward pass, the results are aggregated because intermediate outputs from all participating layers need to be kept in memory until the phase finishes. The memory is therefore composed of intermediate outputs and the computed gradients [28].

There are three main insights. First, given the same batch size, the first layers generally use more memory. Second, an increase in batch size causes a much larger increase in per-layer memory usage in the first layers suggesting these layers are crucial for reducing overall memory consumption. Third, given different batch sizes, the first layers can actually become cheaper (in terms of memory used) than the backward phase, illustrating the potential benefits of adapting the batch size for the first layers.

3.4 Status quo

We illustrate the limitations of the standard approach of running the ML computation entirely in the compute tier while streaming the input images from the COS. We experiment with training with a batch size of 500 images on either CPU or GPU. To show the impact of the limited network bandwidth between the COS and the

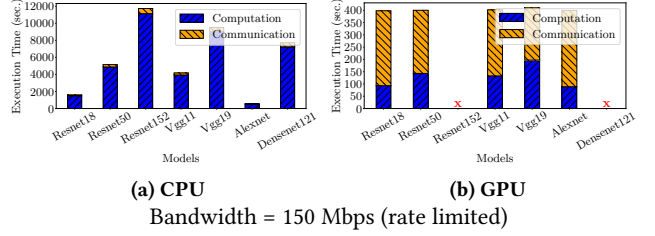


Figure 5: Execution time of Status quo. Dataset: Imagenet. Batch size = 500. 'X' signifies OOM crashes.

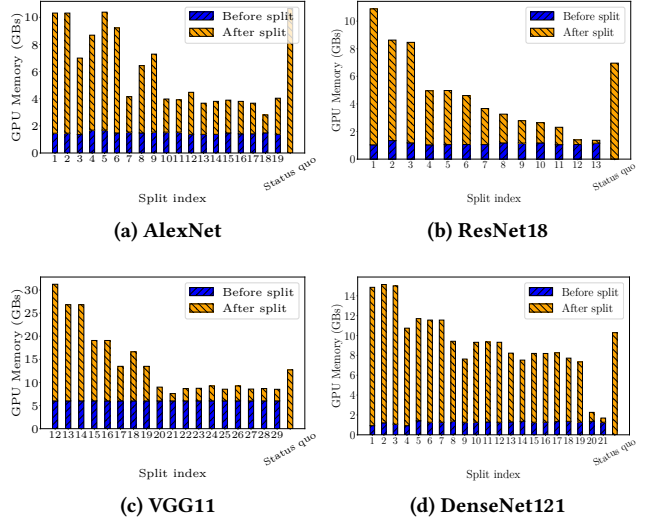


Figure 6: GPU memory breakdown with splitting the forward pass at different layers (x-axis). Dataset: Imagenet.

compute tier, we artificially rate-limit the network bandwidth to 150 Mbps.³

Figure 5 shows the communication-computation breakdown. First, as expected, training on the CPU takes longer than on the GPU. Second, the communication is the bottleneck when training with GPUs because the network transfer rate is far lower than the GPU training speed. A corollary of that is that the GPU is not efficiently utilized, remaining idle while waiting for data, despite having communication and computation overlapped as much as possible. Finally, some of the models crash with out-of-memory (OOM) errors on GPU. Unfortunately, to get around this, practitioners currently can only choose between a set of sub-optimal solutions: use a smaller batch size which could affect the accuracy, move to more expensive GPUs, or run with CPUs which are slow.

As an alternative to the status quo and following our observations in §3.3, Figure 6 shows an example in which we split the forward pass into 2 parts: before the split index (blue), we use a batch size of 100 and after (orange), we use a batch size of 1000. We measure the GPU memory with different split indexes. The

³We intentionally limit the bandwidth to a small value to clarify our point. We experiment with a wide range of bandwidth in §5.4.

main takeaway from the figure is that combining a small batch size before the split with a later split index can greatly reduce the total GPU memory usage, sometimes below that of the status quo, i.e., with no splitting.

To sum up, we need a solution that mitigates the network bottleneck, improves GPU memory utilization, and enables fast ML computations even on CPUs. Our main idea is to split the TL computation among the COS and compute tier.

4 DESIGN AND IMPLEMENTATION

4.1 Main observations

The design of HAPI relies on several observations. First, §3 shows that we can leverage the TL DNN’s structure to split the DNN’s feature extraction phase at a layer that reduces the amount of data sent over the network. Second, splitting the TL computation naturally decouples the batch size of feature extraction from the training batch size and thus allows HAPI to adapt the feature extraction batch size to improve resource efficiency and performance. Third, adapting the feature extraction batch size *does not affect training accuracy* because the training batch size does not change (it is decoupled), and the feature extraction work is deterministic (its weights are frozen). Therefore, the contents and size of training batches do not change. Finally, adapting the feature extraction batch size allows HAPI to greatly reduce the GPU memory and output size of the first few layers of the DNN, making them amenable for executing with the scarce computational resources of the COS. This also enables increased concurrency in the COS.

Limitations of pushing everything in the COS. One could envision pushing down both phases of TL, feature extraction and training, to the COS. This reduces the network traffic to minimum, i.e., no data is transferred during training; only at the end, the user might download the trained model from the COS. Yet, this solution fails to decouple the batch size of feature extraction from that of training, leading to a choice between unsatisfactory options which impact both provider efficiency and user experience: limited COS concurrency, poor throughput, or risk of OOM errors (§5.5).

4.2 Design overview

At the high level. As shown in Figure 7, HAPI has two components: the HAPI client, which runs on the compute tier, and the HAPI server, which runs in the COS. The client decides how to split the DNN. The server performs batch adaptation. On the COS side we differentiate between proxy and storage nodes. This is based on our object store service which employs this two layer design. The HAPI server runs on the COS proxy. There is a fast network between the COS proxy and the COS storage nodes, which host the DNNs and the dataset. However, the network between the compute tier and the COS has limited bandwidth. The COS computation capacity and GPU memory are fixed and limited. Multiple requests from the clients share the COS resources.

Terminology. The DNN layer at which HAPI decides to split the DNN is the *split index*. The *freeze index* is the DNN layer that separates feature extraction from training, and it is chosen by the user. The *training batch size* is the batch size specified by the user, and it is used in the training phase. HAPI might decide to use a

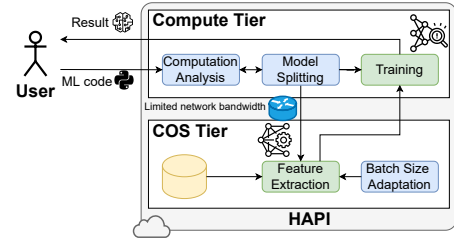


Figure 7: HAPI’s architecture. The client side is in the compute tier, and the server side in the COS.

different batch size for computation on the COS (§4.5); we call this the *COS batch size*. We use *POST request* to refer to a request sent from the HAPI client to the HAPI server. We use *storage request* to refer to a request sent by the HAPI server to the storage nodes.

Request flow. Figure 8 depicts an example of the flow of one request. To initiate a TL computation, users provide their application to the HAPI client, which extracts the application configuration (e.g., the model type, the dataset, the freeze index, etc.) and splits (§4.4) the DNN into 2 parts: one to be executed on the COS and the other to be executed on the compute tier. This splitting decision happens once per TL computation, before its start.

Subsequently, for each training iteration (i.e. the processing of a training batch size of data), the HAPI client sends to the HAPI server HTTP POST requests containing the necessary information: split index, model type, and the name of the object that stores the corresponding data batch. Several such POST requests may be sent during one iteration because one POST request is needed for each object on storage. Therefore, the number of POST requests depends on the ratio between training batch size and the size of the objects on storage (we assume fixed sized objects).

When the HAPI server receives a request, it first reads the object that holds the training data and the specified DNN by sending a *storage request* to the COS storage nodes and then executes the feature extraction part up to the split index. Note that the HAPI server chooses at will the COS batch size to be used for feature extraction (§4.5) depending on the availability of its GPU memory and the concurrent (or to-be-shortly-served) POST requests.

After finishing the feature extraction portion assigned to it, the HAPI server sends back the outputs of the split index layer to the HAPI client, which then uses these outputs to continue the TL computation on the compute tier. Note that the client uses the training batch size for its entire computation even while executing the last part of feature extraction (if any).

Observations. First, HAPI only executes feature extraction next to storage in the COS. Consequently, the split index will be always smaller than or equal to the freeze index (i.e. the split is always before the training phase). Second, the COS batch size is upper bounded by the training batch size as the latter defines the value requested by the user, which we cannot exceed.⁴ Third, scaling down the COS batch size does not affect the convergence of TL as

⁴Practically, we can choose a larger COS batch size than the training batch size. Essentially, the client can prefetch (from the server) more intermediate outputs than the training batch size. However, using a large COS batch size may (a) limit concurrency and (b) cause OOM errors. Therefore, HAPI uses a reduced COS batch size.

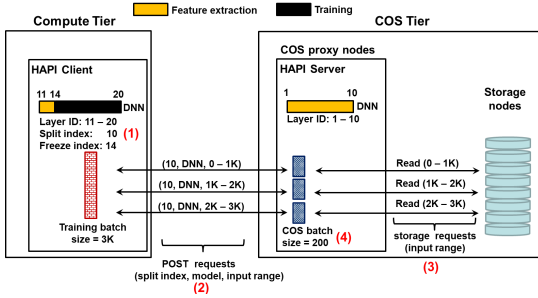


Figure 8: HAPI request flow. A TL job is split at layer 10 with training batch size 3000. 3 requests are sent to the HAPI server. On the COS, for each requests, feature extraction uses COS batch size = 200.

it is used only for feature extraction rather than training. Fourth, since we limit the POST request size, these requests are lightweight and can be executed fast on the COS GPUs. Fifth, there is no strict ordering on the completion of parallel POST requests. Yet, the HAPI client re-orders the intermediate results returned from the server to ensure that the order of data in a training batch does not change, thus maintaining the learning trajectory.

Practical reasons behind the design. The design of HAPI employs lightweight requests and a stateless server in order to address a number of practical concerns. The HAPI server is stateless in the sense that different POST requests, even from the same TL job, are treated independently i.e., they do not reuse images or the model from other requests from the same job. Lightweight requests facilitate load-balancing and help avoid head-of-line blocking where lightweight requests get stuck behind expensive ones. A stateless server simplifies failure recovery as new requests can simply be sent to other servers. A stateless server also simplifies scalability. Scaling the system simply requires adding or removing independent HAPI servers on the COS proxy nodes.

4.3 Efficient client-side profiling

The HAPI server and client require an accurate estimation of the per-layer output sizes and GPU memory usage to drive the batch adaptation (§4.5) and splitting algorithms (§4.4). While the model and layer output sizes are statically known and account for the bulk of GPU memory usage, by themselves they are insufficient for good accuracy because machine learning frameworks (e.g. PyTorch) may not release memory predictably. Therefore, in HAPI we use a hybrid profiling approach, combining statically known information with an inexpensive profiling run.

The HAPI client performs the profiling, once per application before its start. The GPU memory profile is composed of (1) model weights, (2) input data, and (3) intermediate layer outputs generated during the computation. The last two grow proportionally with the batch size, while (1) remains constant. The HAPI client runs a forward pass with a synthesized data sample (same dimensions as input data), keeping track of the per-layer memory consumption and the intermediate layer outputs sizes. A single data sample (i.e., batch size of 1) is sufficient, and hence, profiling is lightweight in terms of both time (few ms) and memory (few MB). After the

profiling run, an estimation of the maximum memory used during the run is computed as the sum of model size and the memory used by the most expensive layer (i.e. maximum input plus output size across all layers). This is compared against the measured maximum memory over the profiling run. Any difference is assumed to grow proportionally with the batch size. We obtain the following prediction errors when extrapolating the maximum GPU memory usage for a batch size of 128MB: ResNet18 0.0005%, ResNet50 6.4%, VGG11 11.7%, VGG19 0.00025%, AlexNet 5.3% and DenseNet121 1.11%.

The HAPI client sends the profiling results to the HAPI server in the specifications of the workload inside every POST request. The HAPI server estimates the memory necessary for its partition of the computation by multiplying the profiled values by the COS batch size which it will calculate (§4.5). Our profiling strategy has several advantages: it is fast, lightweight, agnostic to the model and the DNN layers and it does not rely on pre-computed models which may be based on different hardware. Finally, when the estimation is not perfect, we always over-estimate, thus guarding against OOM.

4.4 Splitting algorithm

The HAPI client runs the splitting algorithm once per application. The algorithm comprises two phases: (1) *candidate selection*, guided purely by model properties and (2) *winner selection*, which selects the best candidate guided by environment properties, namely the network bandwidth to the COS.

Candidate selection (Alg1:9-10) relies on the layer output sizes (§4.3) and chooses layers with output size smaller than the application input size because this reduces network traffic compared to sending the entire application input to the client. In addition, candidate layers cannot come after the freeze layer as we do not push down any part of training to the COS.

Algorithm 1 Choose the split index

```

1: procedure PROFILE_MODEL(model, input_size)
2:   one_input_point=random_tensor(input_size)
3:   intermediate_sizes = forward_pass(model, one_input_point)
4:   model_size = get_size(model)
5:   return intermediate_sizes, model_size

6: procedure CHOOSE_SPLIT_IDX(model, iteration_input, freeze_idx)
7:   input_size = size(iteration_input)/len(iteration_input)
8:   intermediate_sizes, model_size=profile_model(model, input_size)
9:   // candidate selection phase
10:  potential_layers = model.where(intermediate_sizes < input_size and layer_idx
    <= freeze_idx)
11:  // winner selection phase
12:  C = read_network_bandwidth()
13:  winner = freeze_idx
14:  for each layer  $l$  in potential_layers do
15:    if intermediate_sizes[ $l$ ] * model.training_batch_size < C then
16:      winner = intermediate_sizes[ $l$ ]
17:    break
18:  return winner
    
```

Winner selection (Alg:11-18) is a dynamic approach that navigates the trade-off between two potentially opposing needs: (1) to push down as few layers as possible to save COS resource while (2) reducing network communication time to improve user-perceived latency. Key is the insight from §3.1, that layer output size decreases non-monotonically over the DNN. Hence, it is possible to find layers early in the DNN with comparatively small output sizes. To best

navigate this trade-off, the algorithm chooses the earliest candidate layer with an output size (scaled by the training batch size) lower than C where C is a function of the network bandwidth, essentially trading off an optimal splitting point, with respect to network transfers, for reduced pushdown to the COS. In our experiments, we found that a good value for C is network bandwidth times 1s.

To better understand the dynamicity of the algorithm, consider that if the network bandwidth is abundant, the algorithm tends to choose an earlier split point with a comparatively larger output. With limited bandwidth, the split index moves towards latter layers. The training batch size has a similar influence. The larger the batch size is, the larger the layer output sizes become. In this case, the algorithm tends to choose a later split index to compensate since latter layers tend to have comparatively smaller output sizes.

Implementation considerations. The runtime of a request on the server varies greatly depending on the concurrency level and the models both of which change frequently, at the level of seconds, in our design based on lightweight requests. For that reason we avoided incorporating request runtime estimations into the decision process. Finally, because we do not see large variations in the network bandwidth between servers and clients, we do not recalculate the splitting index during the execution of a job.

4.5 Batch adaptation algorithm

This algorithm runs repeatedly at the HAPI server. A new run of the algorithm is triggered when two conditions hold: (1) there is available GPU memory for new requests, and (2) there exists at least one queued request that has not yet been accounted for in the previous runs of the algorithm. Because of HAPI client’s design, it is likely that the HAPI server receives several requests in quick succession. Thus, the HAPI server waits for new requests for a small amount of time. This approach navigates the following trade-off. If the server delays the start of the algorithm too long, this might unnecessarily delay requests. However, if the server does not wait enough, arriving requests might have to wait for the current batch to finish processing (when there is insufficient memory). The algorithm takes into account the already-running requests (i.e., at the time of applying the algorithm) but not the future requests. The goal of the algorithm is to maximize the GPU memory utilization over the existing requests while fitting as many of them inside the GPU memory. The output of the algorithm is the batch size to be used for each request, i.e., the COS batch size.

To choose the batch size for each request, the HAPI server solves the following optimization problem:

$$\begin{aligned} \max \quad & \sum_{r \in \mathcal{R}} b_r \times \mathcal{M}_r(\text{data}) + \mathcal{M}_r(\text{model}) \\ \text{s.t.} \quad & \forall r \in \mathcal{R} \quad b_{r_{min}} \leq b_r \leq b_{r_{max}}, \\ & \sum_{r \in \mathcal{R}} b_r \times \mathcal{M}_r(\text{data}) + \mathcal{M}_r(\text{model}) \\ & \leq \mathcal{M}_{\text{total}} - \mathcal{M}(\text{occupied}), \end{aligned} \quad (1)$$

where \mathcal{R} is the set of requests in the queue, b_r is the batch size for request r (i.e., the decision variables of the optimization problem), $\mathcal{M}_r(\text{data})$ is the GPU memory used by both the input and the intermediate outputs of the DNN for request r , $\mathcal{M}_r(\text{model})$ is the memory used by the DNN weights for request r , $\mathcal{M}_{\text{total}}$ is the total

GPU memory, $\mathcal{M}(\text{occupied})$ is the memory used by other already-running requests in addition to the estimation for the reserved memory for CUDA and the ML framework⁵, and $b_{r_{min}}$, $b_{r_{max}}$ are the minimum and maximum bounds allowed for the batch size. Note that $b_{r_{max}}$ is set by the HAPI client (typically, same as the training batch size) while sending the request, whereas $b_{r_{min}}$ is set by the provider. In our experiments, we set $b_{r_{min}}$ to 25 as we observe that using a smaller batch size would lead to an unnecessary overhead.

We now make a few clarifications. First, the HAPI server distributes requests evenly on the existing GPUs. The batch adaptation algorithm runs separately for each GPU on the COS. Second, since all requests look independent to the server (even when coming from the same user), requests from the same user might be assigned totally different COS batch sizes. Our experiments show that in such small-scale ML computation (i.e., only forward pass with limited amount of data), the COS batch size does not visibly impact the total execution time. Finally, if the server cannot solve the problem it removes one request at a time and retries until a solution is found. The removed requests become part of the next batch assignment round, typically after some existing requests finish.

Implementation considerations. The maximum concurrency allowed by the batch adaptation algorithm is a function of the GPU RAM and the minimum COS batch size. In HAPI the concurrency level is capped statically based on empirical understanding of the overheads resulting from concurrency. Unlucky requests that just miss the last batch adaptation iteration need to wait for the next iteration. We have not seen a significant impact from this.

4.6 End-to-end system

We use a two layer COS and we use PyTorch [49] for ML computation on both the client and server sides.

The HAPI server. We integrated HAPI’s server in COS’s proxy server by adding the batch adaptation algorithm and functions for ML computation. When it receives a POST request, the server reads the object holding the training data from the storage nodes and passes it to the ML function. Each request is served by a separate OS process. On the ML side, we created custom DNN models that run the forward pass between arbitrary start and end layers enabling splitting the computation at any arbitrary layer. We have not yet automated the customization of the models but believe it is possible and plan to do it as future work.

The HAPI client. Apart from choosing the split index, the HAPI client runs the user’s TL code. Two parts of the vanilla training code required changes. First, we use our custom models to enable starting computation from an arbitrary layer instead of the default first layer. Second, we stream the intermediate outputs (of the last layer executed on the COS) using HTTP POST requests instead of streaming the raw training data (with HTTP GET requests). Users provide the same training parameters in both cases, with status quo and HAPI, and hence, the whole process is transparent to them.

Processing costs. As expected, HAPI has cost on top of the actual ML processing done on the GPU. Depending on the model, these costs may outweigh the ML processing cost. Some of the costs exist

⁵This is estimated by the provider before starting the server

in any similar system e.g., moving data to and from GPU. Specific to HAPI are the costs related to serializing and de-serializing the intermediate outputs at the split index.

5 EVALUATION

5.1 Methodology

Applications. HAPI is application-agnostic: its benefits are orthogonal to the training objective, i.e., any TL application that trains a DNN can use HAPI. It can be used for speech recognition [19, 26] or language modelling [7]. In our evaluation, we focus on image classification as our DL application for two reasons: (1) due to its wide use in both academia and industry, and (2) since the data points (i.e., images) used for such applications are large compared to those of other applications (e.g., text or audio files). We train various model families with different sizes, including AlexNet [41], ResNet [27], VGG [56], and Transformer [59]. The latter is a major recent breakthrough. Although originally designed for language modelling tasks, the Transformer model has been proven useful for image classification [38], video understanding [5], and biological sequence analysis [46]. The complete model list along with the default freeze layer is shown in Table 1. Unless otherwise stated, we use the defaults: Imagenet [18] as the dataset, AlexNet as the training model and a training batch size of 2000.

Model	ResNet18	ResNet50	VGG11	VGG19	AlexNet	DenseNet121	Transformer
Freeze Layer	11	21	25	36	17	20	17
Nb of Layers	14	22	28	45	22	22	19

Table 1: Models used in this paper. For DNNs structured as a sequence of blocks (e.g. ResNets) we split at block boundary.

Metrics. We use the following metrics for evaluation.

1. *Execution Time.* The end-to-end latency of executing one epoch of training. Our computation shows that running training for multiple epochs only multiplies this value by a factor.
2. *Transferred Data.* The average amount of data transferred over the network (between the COS and compute tier) per training iteration. One iteration may comprise multiple POST requests to the COS. In addition, one epoch usually comprises multiple iterations.
3. *GPU Memory Consumption.* The maximum amount of GPU memory used, measured periodically using *nvidia-smi*.

HAPI configuration. We divide our dataset into equal-sized chunks of 1000 images, each chunk being one COS object. We choose this object size following recommendations [39] to avoid small requests in order to maximize COS throughput. We set the POST request size to 1000. This has 2 implications: (1) the smallest training batch size we use is 1000, and (2) the number of parallel requests sent by the HAPI client to the COS equals the training batch size divided by 1000. Unless otherwise stated, the default COS batch size is 200. Our batch adaptation algorithm may decide to change this. The minimum COS batch size is 25 because on our hardware smaller batch sizes add unnecessary overhead. Unless otherwise stated, we limit the bandwidth between the HAPI client and the COS to 1 Gbps to reflect the average bandwidth in today’s COS [39, 50]. Nevertheless, we analyze the impact of changing the network bandwidth in §5.4. We use VMs of the same type as in §3. On the COS side we use 1 proxy server and storage uses a replication factor of 3.

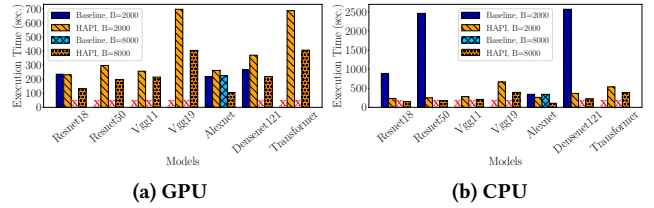


Figure 9: Execution time of BASELINE compared to HAPI with different DNNs. ‘X’ signifies OOM crashes.

Competitors. To the best of our knowledge, HAPI is the first system to split ML computations between the compute tier and the COS. We compare HAPI to a BASELINE that trains solely on the compute tier, streaming as many images as the training batch size from the COS while pipelining streaming and computation. We also compare against a static splitting approach that splits at the freeze layer.

Summary of the findings:

- (1) HAPI improves the execution time compared to BASELINE on both GPUs and CPUs (§5.2).
- (2) HAPI shows benefits across a range of network bandwidths, alleviating the network bottleneck and allowing for faster computation (§5.4).
- (3) HAPI scales well with up to 10 tenants, achieving considerable throughput gain compared to executing the computation entirely on the COS (§5.5).
- (4) HAPI reduces the data transferred over the network, upper bounding it even with large training batch sizes (§5.6).
- (5) HAPI’s batch adaptation algorithm utilizes 100% of the COS GPU memory while preventing OOM errors (§5.7).

5.2 End-to-end experiment

Figure 9 shows the end-to-end execution time of HAPI and BASELINE with 2 training batch sizes and with different models. We experiment with a strong client (i.e., equipped with 2 GPUs) and a weak client that has access only to a CPU.

The first observation is that BASELINE fails to complete the execution in many cases due to out-of-memory (OOM) errors. Even with 64 GB RAM, BASELINE fails to run even the smallest version of VGG networks nor the Transformer model with a batch size of 2000 (Figure 9b). Indeed, the largest training batch size we can use with BASELINE and the Transformer model is only 200, which is an unrealistic value that leads to suboptimal learning. With a batch size of 8000 (the batch size required to train Imagenet for the best accuracy [24]), BASELINE manages to run only AlexNet. This does not happen with HAPI for 2 reasons: (1) the batch adaptation algorithm on the COS reduces the batch size for feature extraction when it realizes that the computation will not fit in the available memory. (2) The actual training part (in the compute tier) requires very little memory and hence, no matter how big the training batch size is, the memory used never reaches the upper limit.

Since HAPI shifts the bottleneck from the communication to computation, increasing the batch size favors HAPI over BASELINE. Using the same batch size, HAPI outperforms BASELINE in all cases

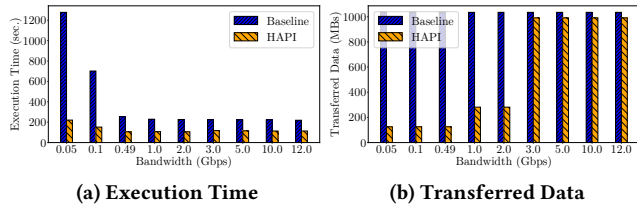


Figure 10: The effect of varying bandwidth on HAPI.

on CPU and for a batch size of 8000 on GPU. For a batch size of 2000 on GPU, BASELINE performs better for AlexNet and DenseNet121. There are several reasons. There is an overhead with HAPI because it needs to load the model twice on server and client sides. Moreover, HAPI handles each request independently and adds another overhead. This overhead is less significant with a batch size of 8000 as more requests are handled in parallel. Overall, HAPI achieves an average execution time speedup of $1.17\times$ (on GPU) and $5.05\times$ (on CPU) and up to $2.13\times$ (on GPU) and $9.95\times$ (on CPU) over BASELINE with a batch size of 2000 and 8000, respectively. Interestingly, in some cases, a weak HAPI client outperforms a strong BASELINE client, a direct benefit of HAPI’s splitting algorithm. For example, training ResNet18 with batch size 2000, on CPU with HAPI takes 232s, whereas on GPU with BASELINE it takes 235s.

Since HAPI is compute bound, the speedup increases with batch size. For example, HAPI’s execution time on AlexNet on GPU drops from 262s to 105s when the batch size increases from 2000 to 8000. For BASELINE increasing the batch size has no effect because the network remains the bottleneck.

5.3 Compared to splitting at the freeze layer

An appealing alternative to HAPI’s dynamic splitting algorithm is a simple static splitting approach that splits at the freeze layer, particularly since Figure 2 indicates that the freeze layer has a greatly reduced output size compared to most layers before it. Interestingly, HAPI can do better by splitting at an earlier layer with a larger output size than the freeze layer. To showcase this we use DenseNet, 4 clients with a training batch size of 2000 and the 12Gbps unrestricted network bandwidth. HAPI decides to split at layer 9 whereas the freeze layer is 20. Despite sending twice the amount of data per iteration over the network, splitting at layer 9 wins (85.86s vs 92.56s) because this reduces the amount of work on the server.

5.4 Impact of network bandwidth

Figure 10 depicts the execution time and data transferred with different values of network bandwidth between the compute tier and the COS. Here, the training batch size is 8000. Figure 10a shows that HAPI outperforms BASELINE in all cases, even with abundant bandwidth ($1.93\times$ faster). HAPI performs even better ($5.79\times$ faster) in extreme cases where the bandwidth is as little as 50 Mbps. HAPI manages to have almost a flat curve along with different values for the bandwidth.

Bandwidth (Gbps)	0.05	0.1	0.5	1	2	3	5	10	12
Split Index	17	17	16	13	13	5	5	5	5

Table 2: The chosen split index by HAPI in Figure 10.

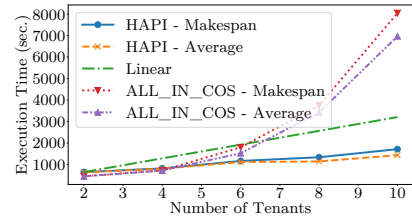


Figure 11: Scalability of HAPI with multi-tenants compared to ALL_IN_COS which pushes down the entire computation.

The key lies in controlling the amount of data transferred in each case (Figure 10b). Up to 2 Gbps, HAPI transfers less than 400 MBs per iteration, whereas BASELINE transfers more than 1 GBs per iteration in all cases. With enough bandwidth (≥ 3 Gbps), HAPI adapts and transfers almost as much as BASELINE. The main knob in such adaptation is the split index. Note that, for HAPI, the transferred data is the output of the last layer executed in the COS. The size of such outputs changes dramatically across layers (§3.1). HAPI carefully chooses the split index depending on the available bandwidth. Table 2 shows the split indexes chosen by HAPI for the different bandwidths in (Gbps). In fact, HAPI chooses the freeze layer (17) as the split index with limited bandwidth, and layer 5 (whose output is still smaller than the raw input images) with abundant bandwidth.

5.5 Scalability on the COS

Figure 11 shows how HAPI scales with multiple tenants. We found that 10 concurrent tenants are sufficient to saturate both GPUs on a COS server. Each tenant submits one request to train a model from Table 1 in round-robin fashion. All requests use a training batch size of 1000 and are submitted at $t=0$. Since the goal of this experiment is to overload a COS server, we do not run actual computation on the client. Figure 11 shows both the makespan (the time to finish all requests) and the average job completion time (JCT). In addition, it compares against the ALL_IN_COS solution (§4.1) in which the entire TL computation is pushed to the COS.

The server can run up to 6 tenants concurrently, finishing all of them almost at the same time. This is visible in the very small difference between the makespan and average JCT. Yet, the scalability of HAPI is not perfect as sharing the GPUs on the COS side has an inevitable overhead. Running 6 concurrent tenants increases the average JCT by $1.7\times$ compared to the case of 2 tenants. With more than 6 tenants, the GPU memory becomes insufficient to fit all the requests so some requests queue waiting for other requests to finish first, i.e., the optimization problem is not solved from the first trial. Consequently, some tenants finish faster than others. For example, the difference between makespan and the average JCT with 10 tenants is 280s. Although ALL_IN_COS achieves comparable results to HAPI with a few tenants, it fails to scale. Compared to ALL_IN_COS, HAPI improves average throughput (based on average JCT) by $2.2\times$ and up to $4.9\times$ with 10 tenants.

Training batch size	1000 - 4000	6000	7000	8000
% of requests with reduced COS batch size	0.0	1.88	15.38	30.0
Average reduction in COS batch size	0.0	1.78	14.51	25.13

Table 3: HAPI’s batch adaptation stats in Figure 13.

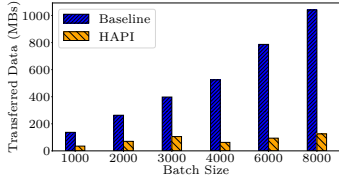


Figure 12: Average data size transferred in one iteration, with HAPI vs. BASELINE, with different batch sizes.

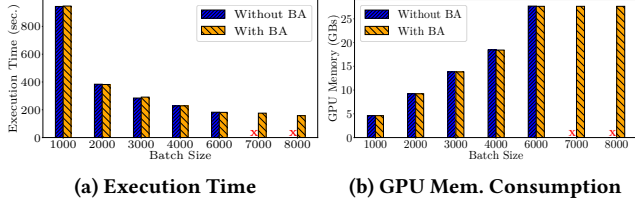


Figure 13: The benefits of batch adaptation (BA).

5.6 Reduction in transferred data

Figure 12 shows the average data size transferred from the COS to the client per training iteration with different training batch sizes. As the training batch size increases, BASELINE streams more data per iteration and hence, we observe a linear increase in the data transferred with the batch size. This in turn increases the execution time linearly especially when the bandwidth is limited.

HAPI keeps the amount of data transferred almost constant with any batch size. The reason is the adaptive choice of the split index. To give a concrete example, notice the decrease in the amount of data transferred despite increasing the batch size from 3000 to 4000. In fact, with a batch size of 3000, HAPI chooses 13 to be the split index, transferring on average 105.6 MBs per iteration. With a batch size of 4000, it chooses 16 to be the split index, transferring 62.6 MBs per iteration. The logic is that with a larger batch size, more data is expected to be transferred from the COS in each training iteration assuming the same split index and network bandwidth. HAPI adapts by choosing a later split index for the increased batch size to try to keep the amount of time spent in network communication comparable. This adaptive behavior alleviates the network bottleneck and makes the whole operation compute bound.

5.7 Batch adaptation

To show the benefits of the batch adaptation (BA) algorithm we run two versions of HAPI: one with BA and one without. We vary the training batch size from 1000 to 8000. Increasing the batch size increases the number of parallel POST requests to the COS since we fix the size of a request to 1000 (e.g. 6 parallel posts for a training batch size of 6000). To overload the GPU memory of the COS, we set the COS batch size to 1000. Figure 13 shows the results while Table 3 complements with: (1) the % of requests whose batch size is reduced by BA, and (2) the average reduction.

Figure 13a shows the execution time, which decreases with increasing batch size. The reason is that the number of training iterations decreases with increased batch size, enabling faster epochs. Up to 6 requests, HAPI achieves the same execution time in both

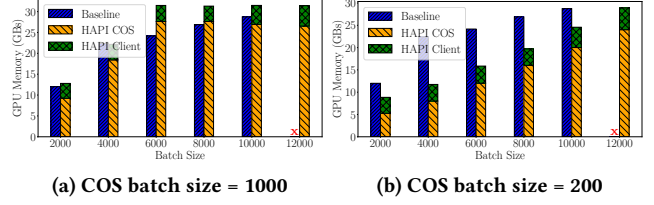


Figure 14: Total GPU memory used in HAPI vs. BASELINE.

cases, indicating that the overhead of BA is negligible with sufficient memory. For more than 6 requests, the GPU memory becomes insufficient, so BA starts reducing the batch size, successfully preventing OOM crashes. The overhead of BA remains very small in these cases, visible in the fact that the execution time remains small with big batch sizes. Precisely, the server takes 25ms to run the BA algorithm once.

Figure 13b shows the memory usage in each case. On the one hand, not using BA increases linearly GPU memory usage with batch size until crashing due to OOM. On the other hand, BA adapts batch size to fit into the existing memory, leveling memory usage for large batch sizes and avoiding OOM. The maximum memory usage is 28GBs and not $2 * 16$ GBs because the remainder is reserved by CUDA and PyTorch.

Figure 13 and Table 3 show the importance of scaling down the COS batch size to avoid OOM errors. For example, with a batch size of 8000, HAPI decided to scale down 2-3 requests on average, with an average COS batch size reduction of around 25%. Put differently, if the COS batch sizes were 25% smaller on average (i.e. 750 instead of 1000), all requests would have fit (theoretically) with no need to adapt the COS batch size. Such information is usually obscure and hard-to-get to the users, leaving them susceptible to choosing a large batch size and crashing the learning procedure.

5.8 Breakdown of memory

Figure 14 shows the GPU memory usage by HAPI (across both compute tier and COS), with 2 COS batch sizes, compared to BASELINE, and using different training batch sizes. The memory usage of BASELINE and HAPI’s client is identical in Figures 14a and 14b; only the COS memory changes.

Figure 14a shows that splitting enables fully utilizing COS GPU memory while giving the impression of extra memory to the user. Precisely, the aggregate GPU memory can exceed 30 GB, which is beyond the capabilities of the user in our setup (e.g., see batch size 12000). This enables the user to train with larger batch sizes.

Figure 14a also shows a source of overhead that appears with sending many parallel requests. There is a slight decrease in the COS GPU memory usage with more than 8 concurrent requests (i.e., batch size > 8000). The reason lies with the *independent* nature of requests, each served by a separate process. Thus, a separate chunk of memory is reserved for each request leaving slightly less room for the actual data. Our memory modeling captures this overhead, making best use of the available memory without OOMs.

In Figure 14b, the COS batch size is small (200). The aggregate memory usage is even less than BASELINE showing the effectiveness of the COS batch size knob.

5.9 Small batch sizes

When fine tuning TL applications, sometimes practitioners use smaller batch sizes compared to training the DNN from scratch. As already discussed in §5, HAPI introduces some overheads that impact the performance for small batch sizes. However, HAPI has an advantage over BASELINE when the latter spends a large portion of time in network communication, i.e., if the network bandwidth is very limited and/or the size of one data point is big. These cases are particularly beneficial for HAPI which performs better in network-bound cases rather than compute-bound.

To illustrate our point with more examples, in the rest of this section, we run experiments with the DNNs with a limited bandwidth of 0.05 Gbps and on half of the Imagenet data (results can be easily extrapolated for the whole data set). In Table 4, we provide the execution times of the DNNs with a training batch size of 512. We can see that for most DNNs, execution times are comparable or better (up to 2.34x better for ResNet50) with HAPI. The Transformer model is not included because, as described in Section 5.2, the largest training batch size we can use with BASELINE and the Transformer model is only 200.

Models	ResNet18	ResNet50	VGG11	AlexNet	DenseNet121
HAPI	619	260	364	283	628
BASELINE	605	609	615	607	614

Table 4: Execution time (in seconds) of BASELINE compared to HAPI with different DNNs. Bandwidth: 0.05 Gbps. Batch size: 512. Dataset: Imagenet.

Moreover, interestingly, we get similar execution times on strong and weak (CPU only) clients. This is due to the fact that as the batch size is small and the computations on CPU are done for the last layers (which are cheaper) only, the time saved by doing the computations on GPU is cancelled by the time spent to move the data to GPU.

The same trends described hold even for smaller batch sizes. For example, when running AlexNet on GPU with a training batch size of 256 and a bandwidth of 0.05 Gbps, HAPI executes in 775 seconds whereas BASELINE executes in 1167 seconds.

We acknowledge that the larger the batch size, the better HAPI is over BASELINE. Moreover, with very small batch sizes and big network bandwidth, if the input data point is not very big, HAPI does not have clear advantage over BASELINE (except for using less GPU memory).

5.10 iNaturalist and PlantLeaves datasets

Next, we present results for the PlantLeaves [55] and iNaturalist [58] datasets introduced in §3. The interesting property of these datasets is that they have an image input size larger than Imagenet’s, which highlights the advantage of HAPI over BASELINE.

The iNaturalist dataset has the image input size roughly double that of Imagenet’s, as shown in Figure 2. The results on iNaturalist

Bandwidths	0.05	0.1	0.5	1	2	3	5	10	12
Speedup	3.63	2.61	1.72	1.57	1.60	1.57	1.49	1.53	1.56

Table 5: HAPI’s speedup for different bandwidths. Dataset: Plantleaves. Batch size: 250.

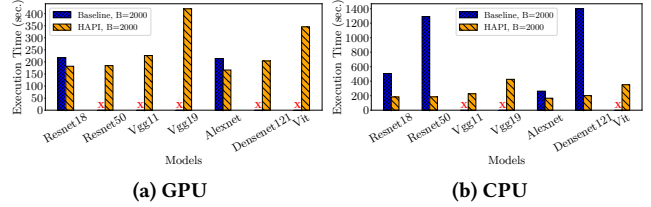


Figure 15: Execution time of BASELINE compared to HAPI with different DNNs. ‘X’ signifies OOM crashes. Dataset: iNaturalist. Batch size: 2000.

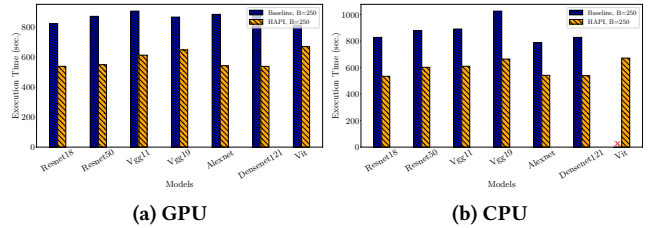


Figure 16: Execution time of BASELINE compared to HAPI with different DNNs. ‘X’ signifies OOM crashes. Dataset: Plantleaves. Batch size: 250.

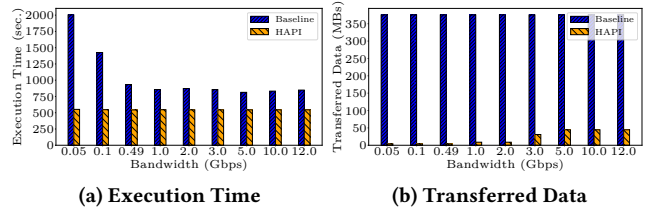


Figure 17: The effect of varying bandwidth on HAPI. Dataset: PlantLeaves. Batch size: 250.

show a similar trend to the ones with Imagenet. As an example, in Figure 15, we show the execution time for iNaturalist with a training batch size of 2000. As in Figure 9, even with a batch size of 2000, most models crash with OOM when running the BASELINE. However, in contrast to Figure 9 where BASELINE performs slightly better or comparable on Alexnet and ResNet18, HAPI now outperforms BASELINE for all the remaining models on GPU and CPU. This is due to the fact that the iNaturalist input size is bigger than Imagenet’s.

The PlantLeaves dataset has an image size roughly eight times larger than Imagenet’s, as shown in Figure 2. Therefore, to show the benefits of HAPI even for small batch sizes and to avoid OOM for fair comparison, we present the results with a training batch size of 250. In Figure 16, we show the execution time of all the DNNs models on CPU and GPU with the PlantLeaves dataset. As expected, even with this small batch size, HAPI outperforms BASELINE in all cases with an average speedup of 1.5, which shows the advantages of using HAPI over BASELINE for bigger input sizes.

Moreover, if we vary the bandwidth between the HAPI client and the COS (as in §5.4), the results for PlantLeaves dataset are similar to Imagenet and are shown in Figure 17. HAPI adapts the split index and the execution time is almost constant for all bandwidths values, whereas it increases drastically for a very limited bandwidth for BASELINE. The speedups per bandwidth value are shown in Table 5. We can notice that even with large bandwidth, using HAPI offers a great reduction in transferred data and better performance as explained above.

6 RELATED WORK

HAPI contains a unique combination of context (COS), workload (TL), and design decisions (splitting a DNN between cloud tiers, batch adaptation). While related work exists in these directions, HAPI is the first to combine them in a single cohesive system.

Batch adaptation in ML. Several projects [54, 57, 66] proposed to dynamically adapt the *training* batch size as training proceeds, leading to shorter training times without loss in accuracy. These ideas are complementary to HAPI’s batch adaptation because they can be applied in HAPI’s training phase. Instead, the key insight of batch adaptation in HAPI is that during the same iteration, it is useful to use different batch sizes for training and feature extraction.

Splitting compute between edge and cloud. Neurosurgeon [37] splits ML *inference* between the cloud and edge devices to achieve low latency, low energy consumption, and high data center throughput. The partitioning is automatic and adapts to dynamics in server load and network bandwidth. Compared to Neurosurgeon, besides considering more complex application (i.e., TL), HAPI dynamically manages storage-side concurrency via batch adaptation. MAUI [15] performs fine-grained (function-level) energy-aware offload of mobile code to the infrastructure, via runtime decisions driven by the goal to save energy. MAUI’s approach to splitting cannot be directly used in HAPI because it requires programmer annotations, and transfers all program state including variables. Odessa [51] offloads stages in perception applications but without analyzing the global impact on application performance.

Offloading compute to storage nodes. Rhea [21] uses static analysis of Java bytecode to generate storage-side filters for Hadoop applications. Rhea shares the goal of mitigating the network bottleneck to storage but targets a different workload, does not split an application and does not optimize the resource utilization in the storage layer. Pyxis [10] uses static analysis and dynamic runtime information to automatically partition a database application between application and storage nodes. Pyxis automatically generates database-side stored procedures to minimize overall latency subject to CPU constraints. For this, it minimizes the number of control transfers as well as amount of data sent during each control transfer. Pyxis differs in the application, context, and concerns (i.e., control transfers are specific to database applications).

Computation pushdown in COS. Work on pushing down computation in the COS mainly focuses on how to best leverage the limited subset of SQL supported by Amazon S3 Select-like systems since 2017. PushdownDB [67] analyzes which DBMS primitives can be cost-effectively moved into S3 and on how more complex operations (e.g., joins) can be re-implemented to take advantage of

S3 Select. FlexPushdownDB [65] combines the benefits of caching and computation pushdown by introducing a separable operator.

Systems challenges for TL. Cartel [16] provides collaborative TL at the edge by transferring knowledge across geographically distributed edge clouds while minimizing transfers over the backhaul network. Cartel differs as it focuses on challenges in learning at the edge, e.g., detecting similarities between edge clouds and performing the knowledge transfer.

Model/pipeline parallelism. Splitting in HAPI is reminiscent of model and pipeline parallelism, which aim to distributedly train large models. Model parallelism [11] splits a DNN across workers. This is a form of intra-batch parallelism as all workers process the same batch. Pipeline parallelism [30, 47] further improves the efficiency of model parallelism. Pipedream [47] combines intra with inter-batch parallelism (multiple batches execute concurrently) and mitigates staleness and consistency issues by keeping several versions of the weights. GPipe [30] does not do inter-batch parallelism, but splits a single batch into micro-batches and pipelines those.

HAPI differs in several ways. The high-level goal differs as HAPI aims to mitigate the COS network bottleneck. The approach to splitting differs as the splitting point in HAPI is dynamic but fixed in model/pipeline parallelism. The concerns differ as HAPI’s server handles multiple clients concurrently. The challenges differ as there is no backpropagation on HAPI’s server or between HAPI’s client and server.

Data ingestion pipelines. The feature extraction phase in HAPI is reminiscent of data ingestion/preparation pipelines [35, 45, 68] because of their goal (data preparation) and the critical focus on efficiently delivering data for training. However, these pipelines are far more general in nature (e.g., can even run user-defined functions [45]) and can be very large (e.g., serve data at TB/s [68]), which makes them unsuitable for running inside the COS. In HAPI, the main difference is that the feature extraction phase is part of the DNN which, while limiting the knobs available, allows us to focus on accelerating each separate application.

7 CONCLUDING REMARKS

HAPI is a transfer learning (TL) processing system that spans the compute and COS tiers. HAPI leverages the unique structure of TL’s fine-tuning phase to mitigate the cloud network bottleneck and maximize the use of the scarce computational resources inside the COS. The key enabler is to carefully split the TL application during feature extraction. This can reduce network transfers and, crucially, decouples the training and feature extraction phases, facilitating the use of batch size adaptation in the COS. We show up to 11× improvement in application runtime and up to 8.3× reduction in data transfers while using 100% of the COS GPU memory.

REFERENCES

- [1] Amazon. Amazon S3. <https://aws.amazon.com/s3/>. Last accessed: Nov, 2022.
- [2] Amazon AQUA. AWS Advanced Query Accelerator. <https://aws.amazon.com/r edshift/features/aqua/>.
- [3] Michael Armbrust, Tathagata Das, Liwen Sun, Burak Yavuz, Shixiong Zhu, Mukul Murthy, Joseph Torres, Herman van Hovell, Adrian Ionescu, Alicja Luszczak, et al. Delta lake: high-performance acid table storage over cloud object stores. *Proceedings of the VLDB Endowment*, 13(12):3411–3424, 2020.
- [4] Amazon AWS. Use pre-trained financial language models for transfer learning in Amazon SageMaker JumpStart. <https://aws.amazon.com/blogs/machine->

- learning/use-pre-trained-financial-language-models-for-transfer-learning-in-amazon-sagemaker-jumpstart/.
- [5] Gedas Bertasius, Heng Wang, and Lorenzo Torresani. Is space-time attention all you need for video understanding. *arXiv preprint arXiv:2102.05095*, 2(3):4, 2021.
 - [6] AWS News Blog. S3 Select and Glacier Select – Retrieving Subsets of Objects. <https://aws.amazon.com/blogs/aws/s3-glacier-select/>. Last accessed: Nov, 2022.
 - [7] Tom B Brown, Benjamin Mann, Nick Ryder, Melanie Subbiah, Jared Kaplan, Prafulla Dhariwal, Arvind Neelakantan, Pranav Shyam, Girish Sastry, Amanda Askell, et al. Language models are few-shot learners. *arXiv preprint arXiv:2005.14165*, 2020.
 - [8] Brad Calder, Ju Wang, Aaron Ogus, Niranjan Nilakantan, Arild Skjolsvold, Sam McKelvie, Yikang Xu, Shashwat Srivastav, Jiesheng Wu, Huseyin Simitci, Jaidev Haridas, Chakravarthy Uddaraji, Hemal Khatrui, Andrew Edwards, Vaman Bedekar, Shane Mainali, Rafay Abbasi, Arpit Agarwal, Mian Fahim ul Haq, Muhammad Ikram ul Haq, Deepali Bhardwaj, Sowmya Dayanand, Anitha Adusumilli, Marvin McNett, Sriram Sankaran, Kavitha Manivannan, and Leonidas Rigas. Windows azure storage: A highly available cloud storage service with strong consistency. In *Proceedings of the Twenty-Third ACM Symposium on Operating Systems Principles, SOSP '11*, page 143–157, New York, NY, USA, 2011. Association for Computing Machinery.
 - [9] Chan Jung Chang, Jerry Chou, Yu-Ching Chou, and I-Hsin Chung. Ecs2: A fast erasure coding library for gpu-accelerated storage systems with parallel & direct io. In *2020 IEEE International Conference on Cluster Computing (CLUSTER)*, 2020.
 - [10] Alvin Cheung, Samuel Madden, Owen Arden, and Andrew C Myers. Automatic partitioning of database applications. *Proceedings of the VLDB Endowment*, 5(11):1471–1482, 2012.
 - [11] Trishul Chilimbi, Yutaka Suzue, Johnson Apacible, and Karthik Kalyanaraman. Project adam: Building an efficient and scalable deep learning training system. In *11th USENIX Symposium on Operating Systems Design and Implementation (OSDI 14)*, pages 571–582, Broomfield, CO, October 2014. USENIX Association.
 - [12] Dooseop Choi, Taeg-Hyun An, Kyoungwan Ahn, and Jeongdan Choi. Driving experience transfer method for end-to-end control of self-driving cars. *arXiv preprint arXiv:1809.01822*, 2018.
 - [13] Alibaba Cloud. Real-Time Image Processing by Object Storage Service . https://www.alibabacloud.com/blog/real-time-image-processing-by-object-storage-service_597996. Last accessed: Nov, 2022.
 - [14] McKinsey & Company. Edlich, Alex, et al. Driving impact at scale from automation and AI. <https://mck.co/3IQIBVi>, page 12.
 - [15] Eduardo Cuervo, Aruna Balasubramanian, Dae-ki Cho, Alec Wolman, Stefan Saroiu, Ranveer Chandra, and Paramvir Bahl. Maui: Making smartphones last longer with code offload. In *ACM MobiSys 2010*, June 2010.
 - [16] Harshit Daga, Patrick K. Nicholson, Ada Gavrilovska, and Diego Lugones. Cartel: A system for collaborative transfer learning at the edge. In *Proceedings of the ACM Symposium on Cloud Computing, SoCC '19*, page 25–37, New York, NY, USA, 2019. Association for Computing Machinery.
 - [17] Microsoft Azure Databricks. Featurization for transfer learning. <https://docs.microsoft.com/en-us/azure/databricks/applications/machine-learning/preprocess-data/transfer-learning-tensorflow>.
 - [18] Jia Deng, Wei Dong, Richard Socher, Li-Jia Li, Kai Li, and Li Fei-Fei. Imagenet: A large-scale hierarchical image database. In *2009 IEEE conference on computer vision and pattern recognition*, pages 248–255. IEEE, 2009.
 - [19] Onno Eberhard and Torsten Zesch. Effects of layer freezing on transferring a speech recognition system to under-resourced languages. In *Proceedings of the 17th Conference on Natural Language Processing (KONVENS 2021)*, pages 208–212, 2021.
 - [20] Yixiao Gao, Qiang Li, Lingbo Tang, Yongqing Xi, Pengcheng Zhang, Wenwen Peng, Bo Li, Yaohui Wu, Shaozong Liu, Lei Yan, Fei Feng, Yan Zhuang, Fan Liu, Pan Liu, Xingkui Liu, Zhongjie Wu, Junping Wu, Zheng Cao, Chen Tian, Jinbo Wu, Jiayi Zhu, Haiyong Wang, Dennis Cai, and Jiesheng Wu. When cloud storage meets RDMA. In *18th USENIX Symposium on Networked Systems Design and Implementation (NSDI 21)*, pages 519–533. USENIX Association, April 2021.
 - [21] Christos Gkantsidis, Dimitrios Vytiniotis, Orion Hodson, Dushyanth Narayanan, Florin Dinu, and Ant Rowstron. Rhea: automatic filtering for unstructured cloud storage. In *10th USENIX Symposium on Networked Systems Design and Implementation (NSDI '13)*. USENIX, April 2013.
 - [22] Ian Goodfellow, Yoshua Bengio, and Aaron Courville. *Deep learning*. MIT press, 2016.
 - [23] Google. Google Cloud Storage. <https://cloud.google.com/storage>. Last accessed: Nov, 2022.
 - [24] Priya Goyal, Piotr Dollár, Ross Girshick, Pieter Noordhuis, Lukasz Wesolowski, Aapo Kyrola, Andrew Tulloch, Yangqing Jia, and Kaiming He. Accurate, large minibatch sgd: Training imagenet in 1 hour. *arXiv preprint arXiv:1706.02677*, 2017.
 - [25] Walker Haddock, Matthew L Curry, Purushotham V Bangalore, and Anthony Skjellum. Gpu erasure coding for campaign storage. In *International Conference on High Performance Computing*, 2017.
 - [26] Awni Hannun, Carl Case, Jared Casper, Bryan Catanzaro, Greg Diamos, Erich Elsen, Ryan Prenger, Sanjeev Sathesh, Shubho Sengupta, Adam Coates, et al. Deep speech: Scaling up end-to-end speech recognition. *arXiv preprint arXiv:1412.5567*, 2014.
 - [27] Kaiming He, Xiangyu Zhang, Shaoqing Ren, and Jian Sun. Deep residual learning for image recognition. In *Proceedings of the IEEE conference on computer vision and pattern recognition*, pages 770–778, 2016.
 - [28] Robert Hecht-Nielsen. Theory of the backpropagation neural network. In *Neural networks for perception*, pages 65–93. Elsevier, 1992.
 - [29] Gao Huang, Zhuang Liu, Laurens Van Der Maaten, and Kilian Q Weinberger. Densely connected convolutional networks. In *Proceedings of the IEEE conference on computer vision and pattern recognition*, pages 4700–4708, 2017.
 - [30] Yanping Huang, Youlong Cheng, Ankur Bapna, Orhan Firat, Mia Xu Chen, Dehao Chen, HyoukJoong Lee, Jiquan Ngiam, Quoc V. Le, Yonghui Wu, and Zhiheng Chen. *GPipe: Efficient Training of Giant Neural Networks Using Pipeline Parallelism*. Curran Associates Inc., Red Hook, NY, USA, 2019.
 - [31] Huawei. Huawei ECS. <https://www.huaweicloud.com/intl/en-us/product/ecs.html>. Last accessed: Nov, 2022.
 - [32] Huawei. Huawei Object Storage Service (OBS). <https://www.huaweicloud.com/intl/en-us/product/obs.html>. Last accessed: Nov, 2022.
 - [33] IBM. IBM Storage supports NVIDIA DGX A100 AI infrastructure. <https://www.ibm.com/blogs/systems/ibm-storage-supports-nvidia-dgx-a100-ai-infrastructure/>. Last accessed: Nov, 2022.
 - [34] IBM. Optimize running NVIDIA GPU-enabled AI workloads with data orchestration solution. <https://community.ibm.com/community/user/storage/blogs/pallavi-galgali/2020/10/05/optimize-running-nvidia-gpu-enabled-ai-workloads-w?CommunityKey=1142f81e-95e4-4381-95d0-7977f20d53fa&tab=recentcommunityblogsdashboard>. Last accessed: Nov, 2022.
 - [35] Alexander Isenko, Ruben Mayer, Jedele Jeffrey, and Hans-Arno Jacobsen. *Where Is My Training Bottleneck? Hidden Trade-Offs in Deep Learning Preprocessing Pipelines*. Association for Computing Machinery, New York, NY, USA, 2022.
 - [36] Yimin Jiang, Yibo Zhu, Chang Lan, Bairen Yi, Yong Cui, and Chuanxiong Guo. A unified architecture for accelerating distributed DNN training in heterogeneous GPU/CPU clusters. In *14th USENIX Symposium on Operating Systems Design and Implementation (OSDI 20)*, pages 463–479. USENIX Association, November 2020.
 - [37] Yiping Kang, Johann Hauswald, Cao Gao, Austin Rovinski, Trevor Mudge, Jason Mars, and Lingjia Tang. Neurosurgeon: Collaborative intelligence between the cloud and mobile edge. *ACM SIGARCH Computer Architecture News*, 45(1):615–629, 2017.
 - [38] Salman Khan, Muzammal Naseer, Munawar Hayat, Syed Waqas Zamir, Fahad Shahbaz Khan, and Mubarak Shah. Transformers in vision: A survey. *ACM Computing Surveys (CSUR)*, 2021.
 - [39] Ana Klimovic, Yawen Wang, Christos Kozyrakis, Patrick Stuedi, Jonas Pfefferle, and Animesh Trivedi. Understanding ephemeral storage for serverless analytics. In *2018 USENIX Annual Technical Conference (USENIX ATC 18)*, 2018.
 - [40] Gunjae Koo, Kiran Kumar Matam, Te I, H.V. Krishna Giri Narra, Jing Li, Hung-Wei Tseng, Steven Swanson, and Murali Annavam. Summarizer: Trading communication with computing near storage. In *2017 50th Annual IEEE/ACM International Symposium on Microarchitecture (MICRO)*, 2017.
 - [41] Alex Krizhevsky, Ilya Sutskever, and Geoffrey E Hinton. Imagenet classification with deep convolutional neural networks. *Advances in neural information processing systems*, 25:1097–1105, 2012.
 - [42] George Leopold. Nvidia buys object storage vendor swiftstack. <https://www.entrepreneur.com/news/2020/03/06/nvidia-buys-object-storage-vendor-swiftstack/>.
 - [43] Jing Li, Hung-Wei Tseng, Chunbin Lin, Yannis Papakonstantinou, and Steven Swanson. Hippogriffdb: Balancing i/o and gpu bandwidth in big data analytics. *Proceedings of the VLDB Endowment*, 9(14):1647–1658, 2016.
 - [44] Kunal Lillaney, Vasily Tarasov, David Pease, and Randal Burns. The case for dual-access file systems over object storage. In *11th USENIX Workshop on Hot Topics in Storage and File Systems (HotStorage 19)*, 2019.
 - [45] Derek G. Murray, Jiří Šimša, Ana Klimovic, and Ihor Indyk. Tf.data: A machine learning data processing framework. *Proc. VLDB Endow.*, 14(12):2945–2958, jul 2021.
 - [46] Ananthan Nambiar, Maeve Heflin, Simon Liu, Sergei Maslov, Mark Hopkins, and Anna Ritz. Transforming the language of life: Transformer neural networks for protein prediction tasks. In *Proceedings of the 11th ACM International Conference on Bioinformatics, Computational Biology and Health Informatics*, pages 1–8, 2020.
 - [47] Deepak Narayanan, Aaron Harlap, Amar Phanishayee, Vivek Seshadri, Nikhil R. Devanur, Gregory R. Ganger, Phillip B. Gibbons, and Matei Zaharia. Pipedream: Generalized pipeline parallelism for dnn training. In *Proceedings of the 27th ACM Symposium on Operating Systems Principles, SOSP '19*, page 1–15, New York, NY, USA, 2019. Association for Computing Machinery.
 - [48] NVIDIA. GPUDirect Storage: A Direct Path Between Storage and GPU Memory. <https://developer.nvidia.com/blog/gpudirect-storage/>. Last accessed: Nov, 2022.
 - [49] Adam Paszke, Sam Gross, Francisco Massa, Adam Lerer, James Bradbury, Gregory Chanan, Trevor Killeen, Zeming Lin, Natalia Gimelshein, Luca Antiga, et al. Pytorch: An imperative style, high-performance deep learning library. *Advances in neural information processing systems*, 32:8026–8037, 2019.

- [50] Qifan Pu, Shivaram Venkataraman, and Ion Stoica. Shuffling, fast and slow: Scalable analytics on serverless infrastructure. In *16th USENIX Symposium on Networked Systems Design and Implementation (NSDI 19)*, pages 193–206, Boston, MA, February 2019. USENIX Association.
- [51] Moo-Ryong Ra, Anmol Sheth, Lily Mummert, Padmanabhan Pillai, David Wetherall, and Ramesh Govindan. Odessa: Enabling interactive perception applications on mobile devices. In *Proceedings of the 9th International Conference on Mobile Systems, Applications, and Services, MobiSys '11*, page 43–56, New York, NY, USA, 2011. Association for Computing Machinery.
- [52] Maithra Raghu, Chiyuan Zhang, Jon Kleinberg, and Samy Bengio. Transfusion: Understanding transfer learning for medical imaging. In *Advances in Neural Information Processing Systems*. Curran Associates, Inc., 2019.
- [53] Samsung. Samsung V-NAND SSD 980 PRO with Heatsink 2021 Data Sheet. https://semiconductor.samsung.com/resources/data-sheet/Samsung_NVMe_SSD_980_PRO_with_Heatsink_Datasheet_211101.pdf. Last accessed: Nov, 2022.
- [54] V. Saxena, K. R. Jayaram, S. Basu, Y. Sabharwal, and A. Verma. Effective elastic scaling of deep learning workloads. In *2020 28th International Symposium on Modeling, Analysis, and Simulation of Computer and Telecommunication Systems (MASCOTS)*, pages 1–8, Los Alamitos, CA, USA, nov 2020. IEEE Computer Society.
- [55] SC Siddharth, UP Singh, A Kaul, and S Jain. A database of leaf images: practice towards plant conservation with plant pathology. *Mendeley Data*, 2019.
- [56] Karen Simonyan and Andrew Zisserman. Very deep convolutional networks for large-scale image recognition. *arXiv preprint arXiv:1409.1556*, 2014.
- [57] Samuel L. Smith, Pieter-Jan Kindermans, and Quoc V. Le. Don't decay the learning rate, increase the batch size. In *International Conference on Learning Representations*, 2018.
- [58] Grant Van Horn, Oisin Mac Aodha, Yang Song, Yin Cui, Chen Sun, Alex Shepard, Hartwig Adam, Pietro Perona, and Serge Belongie. The inaturalist species classification and detection dataset. In *The IEEE Conference on Computer Vision and Pattern Recognition (CVPR)*, June 2018.
- [59] Ashish Vaswani, Noam Shazeer, Niki Parmar, Jakob Uszkoreit, Llion Jones, Aidan N Gomez, Lukasz Kaiser, and Illia Polosukhin. Attention is all you need. *Advances in neural information processing systems*, 30, 2017.
- [60] Yaqing Wang, Quanming Yao, James T Kwok, and Lionel M Ni. Generalizing from a few examples: A survey on few-shot learning. *ACM Computing Surveys (CSUR)*, 53(3):1–34, 2020.
- [61] Karl Weiss, Taghi M Khoshgoftaar, and DingDing Wang. A survey of transfer learning. *Journal of Big data*, 3(1):1–40, 2016.
- [62] Shuotao Xu, Thomas Bourgeat, Tianhao Huang, Hojun Kim, Sungjin Lee, and Arvind Arvind. Aquoman: An analytic-query offloading machine. In *2020 53rd Annual IEEE/ACM International Symposium on Microarchitecture (MICRO)*, pages 386–399. IEEE, 2020.
- [63] Siyu Yan, Xiaoliang Wang, Xiaolong Zheng, Yinben Xia, Derui Liu, and Weishan Deng. Acc: Automatic ecn tuning for high-speed datacenter networks. In *Proceedings of the 2021 ACM SIGCOMM 2021 Conference, SIGCOMM '21*, page 384–397, New York, NY, USA, 2021. Association for Computing Machinery.
- [64] Jian Yang, Juno Kim, Morteza Hoseinzadeh, Joseph Izraelevitz, and Steve Swanson. An empirical guide to the behavior and use of scalable persistent memory. In *18th USENIX Conference on File and Storage Technologies (FAST 20)*, pages 169–182, Santa Clara, CA, February 2020. USENIX Association.
- [65] Yifei Yang, Matt Youill, Matthew Woicik, Yizhou Liu, Xiangyao Yu, Marco Serafini, Ashraf Aboulnaga, and Michael Stonebraker. Flexpushdowndb: hybrid pushdown and caching in a cloud dbms. *Proceedings of the VLDB Endowment*, 2021.
- [66] Peifeng Yin, Ping Luo, and Taiga Nakamura. Small batch or large batch? gaussian walk with rebound can teach. In *Proceedings of the 23rd ACM SIGKDD International Conference on Knowledge Discovery and Data Mining, KDD '17*, page 1275–1284, New York, NY, USA, 2017. Association for Computing Machinery.
- [67] Xiangyao Yu, Matt Youill, Matthew Woicik, Abdurrahman Ghanem, Marco Serafini, Ashraf Aboulnaga, and Michael Stonebraker. Pushdowndb: Accelerating a dbms using s3 computation. In *2020 IEEE 36th International Conference on Data Engineering (ICDE)*, pages 1802–1805. IEEE, 2020.
- [68] Mark Zhao, Niket Agarwal, Aarti Basant, Bugra Gedik, Satadru Pan, Mustafa Ozdal, Rakesh Komuravelli, Jerry Pan, Tianshu Bao, Haowei Lu, et al. Understanding and co-designing the data ingestion pipeline for industry-scale recsys training. *arXiv preprint arXiv:2108.09373*, 2021.
- [69] Fuzhen Zhuang, Zhiyuan Qi, Keyu Duan, Dongbo Xi, Yongchun Zhu, Hengshu Zhu, Hui Xiong, and Qing He. A comprehensive survey on transfer learning. *CoRR*, abs/1911.02685, 2019.